STAT3 and STAT1 mediate IL-11–dependent and inflammation-associated gastric tumorigenesis in gp130 receptor mutant mice

Matthias Ernst,[1] Meri Najdovska,[2] Dianne Grail,[1] Therese Lundgren-May,[1] Michael Buchert,[1] Hazel Tye,[2] Vance B. Matthews,[1] Jane Armes,[3] Prithi S. Bhathal,[4] Norman R. Hughes,[4] Eric G. Marcusson,[5] James G. Karras,[5] Songqing Na,[6] Jonathon D. Sedgwick,[6] Paul J. Hertzog,[2] and Brendan J. Jenkins[1,2]

[1]Ludwig Institute for Cancer Research, Royal Melbourne Hospital, Melbourne, Victoria, Australia. [2]Centre for Functional Genomics and Human Disease, Monash Institute of Medical Research, Monash University, Clayton, Victoria, Australia. [3]Mater Health Services, Raymond Terrace, South Brisbane, Queensland, Australia. [4]Department of Pathology, University of Melbourne, Melbourne, Victoria, Australia. [5]Isis Pharmaceuticals, Carlsbad, California, USA. [6]Eli Lilly and Co., Indianapolis, Indiana, USA.

Deregulated activation of STAT3 is frequently associated with many human hematological and epithelial malignancies, including gastric cancer. While exaggerated STAT3 signaling facilitates an antiapoptotic, proangiogenic, and proproliferative environment for neoplastic cells, the molecular mechanisms leading to STAT3 hyperactivation remain poorly understood. Using the *gp130*$^{Y757F/Y757F}$ mouse model of gastric cancer, which carries a mutated gp130 cytokine receptor signaling subunit that cannot bind the negative regulator of cytokine signaling SOCS3 and is characterized by hyperactivation of the signaling molecules STAT1 and STAT3, we have provided genetic evidence that IL-11 promotes chronic gastric inflammation and associated tumorigenesis. Expression of IL-11 was increased in gastric tumors in *gp130*$^{Y757F/Y757F}$ mice, when compared with unaffected gastric tissue in wild-type mice, while *gp130*$^{Y757F/Y757F}$ mice lacking the IL-11 ligand–binding receptor subunit (IL-11Rα) showed normal gastric STAT3 activation and IL-11 expression and failed to develop gastric tumors. Furthermore, reducing STAT3 activity in *gp130*$^{Y757F/Y757F}$ mice, either genetically or by therapeutic administration of STAT3 antisense oligonucleotides, normalized gastric IL-11 expression and alleviated gastric tumor burden. Surprisingly, the genetic reduction of STAT1 expression also reduced gastric tumorigenesis in *gp130*$^{Y757F/Y757F}$ mice and coincided with reduced gastric inflammation and IL-11 expression. Collectively, our data have identified IL-11 as a crucial cytokine promoting chronic gastric inflammation and associated tumorigenesis mediated by excessive activation of STAT3 and STAT1.

Introduction

Gastric cancer (GC) is the second most common cause of cancer-related deaths worldwide (1). Although the molecular mechanisms underlying the pathogenesis of GC remain to be fully defined, a causal correlation has been established between GC and chronic inflammation triggered by the Gram-negative bacterium *Helicobacter pylori* (2), which colonizes the epithelium of the gastric mucosa. Meanwhile, several genetic factors have also been linked to GC, including accumulation of (epi-)genetic alterations in *p53* (3), *tff1* (4), *E-cadherin* (5), and *Cox2* (6), as well as genes encoding components of the TGF-β/Smad signaling cascade (7–10). More recently, persistent activation of the latent STAT3 has been proposed as a prognostic factor for poor survival of GC patients (11), while excessive STAT3 activation promotes the growth and survival of gastric cells (12, 13) and is associated with increased gastric angiogenesis (11). These observations are consistent with the capacity of STAT3 to induce expression of genes that promote angiogenesis (e.g., *Vegf*), cell-cycle progression (e.g., *cyclin D1*), and cell survival (e.g., *Bcl-xL*, *survivin*) (14, 15). Although no mutations have been identified in the human *STAT3* gene, persistent STAT3 activity is associated with numerous hematologic malignancies and tumors of epithelial origin (11, 12, 14–16). This suggests that other (epi-)genetic events along the STAT3 signaling cascade(s) cause its activation, including oversupply of ligands for STAT3-activating cytokine or tyrosine (Y) kinase receptors. In this respect, elevated expression of IL-11, a member of the IL-6 cytokine family that activates STAT3, is a recurrent finding in human GC (17).

Besides IL-11, the IL-6 cytokine family comprises IL-27, IL-31, leukemia inhibitory factor (LIF), oncostatin M (OSM), and ciliary neurotrophic factor (CNTF), among others, and plays a crucial role in hematopoiesis, the immune response, inflammation, and cancer (18–20). IL-6 family cytokines execute their actions via the common signal-transducing receptor β-subunit gp130. In particular, binding of IL-6 or IL-11 to their specific receptor α-subunits, IL-6Rα and IL-11Rα, respectively, induces gp130 homodimerization, while other family members engage heterodimeric receptor complexes comprising gp130 and either the LIF receptor, OSM receptor, or WSX-1 β-subunits (21). Ligand-induced β-subunit dimerization subsequently activates receptor-associated JAK, leading to phosphorylation of cytoplasmic Y residues (22). Phosphor-

Nonstandard abbreviations used: ASO, antisense oligonucleotide; GC, gastric cancer; LIF, leukemia inhibitory factor; MEF, mouse embryonic fibroblast.

Conflict of interest: E.G. Marcusson and S. Na are employees of Eli Lilly and Company, Isis Pharmaceuticals, and the Wood Hudson Cancer Research Laboratory, a nonprofit research organization supported in part by a grant from Eli Lilly and Company. J.G. Karras has direct ownership of equity in Isis Pharmaceuticals and has received income from Isis Pharmaceuticals and Altair Therapeutics within the last year. J.D. Sedgwick is an employee of Eli Lilly and Company and holds stock and stock options in that company. All other authors have declared that no conflict of interest exists.

Citation for this article: *J. Clin. Invest.* **118**:1727–1738 (2008). doi:10.1172/JCI34944.

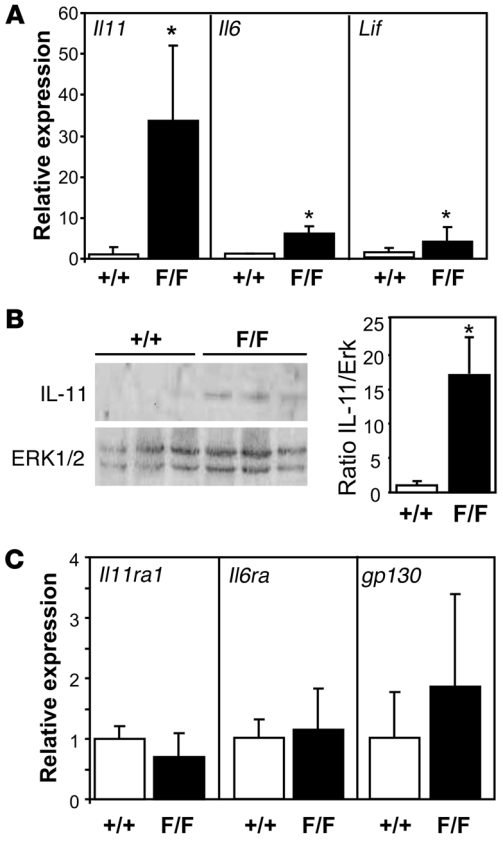

Figure 1
Increased expression of IL-11 and other gp130 family cytokines in gastric tumors of *gp130*$^{Y757F/Y757F}$ mice. (**A**) Quantitative RT-PCR (Q-PCR) analyses of *Il11*, *Il6*, and *Lif* gene expression were performed on cDNA derived from total RNA prepared from antral gastric tissue of 14-week-old *gp130*$^{+/+}$ wild-type (+/+) and *gp130*$^{Y757F/Y757F}$ (F/F) mice. Expression data from 3–5 samples per genotype following normalization for *18S* expression are shown and are presented from replicate analysis as the mean fold induction ± SD relative to expression observed in *gp130*$^{+/+}$ samples. (**B**) Immunoblot analyses were performed on lysates prepared from antral gastric tissue of *gp130*$^{+/+}$ and *gp130*$^{Y757F/Y757F}$ mice using the indicated antibodies. Each lane represents tissue from an individual mouse. Densitometric quantitation of IL-11 in each of 3 representative samples per genotype was performed and normalized against ERK1/2 protein levels. Data are presented as the mean fold induction ± SD relative to expression in *gp130*$^{+/+}$ samples. (**C**) Q-PCR gene expression analyses of *Il6ra*, *Il11ra1*, and *gp130* as in **A**. **P* < 0.05 versus expression in *gp130*$^{+/+}$ samples.

ylation of the 4 carboxyterminal Y residues in gp130 is required and sufficient for the activation of STAT3 and to a lesser extent of STAT1 (23). Meanwhile, the membrane-proximal phosphorylated Y residue in gp130 (pY757 in mouse, pY759 in human) provides a binding site for the tyrosine phosphatase Shp2 (24), which upon phosphorylation mediates activation of the Ras/ERK and PI3K/Akt pathways (25).

We have previously demonstrated the physiological importance of tightly regulated gp130 signaling by STAT3-mediated transcriptional induction of the negative regulator SOCS3, which competes with Shp2 for binding to pY757/pY759 in gp130 (26). In particular, mice homozygous for a phenylalanine (F) knockin substitution of Y757 (*gp130*$^{Y757F/Y757F}$) spontaneously develop gastric hyperplasia characterized by the presence of distinct tumors in the antropyloric region of the glandular stomach, with histological features reminiscent of intestinal-type, metaplastic gastric tumors in humans (27). The molecular consequences of the Y757F substitution mutation, which simultaneously abolishes binding of SOCS3 and Shp2 to gp130, are exaggerated activation of STAT3 and STAT1 (14) and impaired activation of the Shp2/Ras/ERK and Shp2/PI3K pathways (27). We previously proposed a molecular mechanism whereby tumor formation is initiated through impaired expression of the Shp2/Ras/ERK target and gastric tumor suppressor gene *tff1* (27). Meanwhile, the progressive growth of macroscopic lesions depends on STAT3 hyperactivation, because reduction of the pool of cellular STAT3 available for activation by monoallelic gene ablation alleviates gastric tumorigenesis in the corresponding *gp130*$^{Y757F/Y757F}$*Stat3*$^{+/-}$ compound mutant mice (14). The latter effect was partially attributed to the impairment of TGF-β–mediated cytostatic effects that arise from the transcriptional induction of *Smad7* by STAT3 hyperactivation (14). Smad7, a key negative regulator of TGF-β–mediated signaling (28), is also induced by excessive STAT1 activation, which is associated with chronic infection with the gastric class I carcinogen *H. pylori* (29).

Our observation reported here of marked gastric overexpression of IL-11 in *gp130*$^{Y757F/Y757F}$ mice parallels recurrent observations of elevated IL-11 levels in human GC (17) and suggests that IL-11 may be the primary gp130-acting cytokine causing gastric tumorigenesis. Indeed, our present findings that gastric inflammation, hyperplasia, and tumor formation are suppressed in IL-11–unresponsive *gp130*$^{Y757F/Y757F}$*Il11ra1*$^{-/-}$ compound mutant mice coincides with normalized activation of STAT3 and its target genes. Furthermore, genetic as well as pharmacological strategies to specifically reduce STAT3 activation in *gp130*$^{Y757F/Y757F}$ mice impaired gastric IL-11 expression and prevented the growth of gastric tumors. In addition, we also uncovered a hitherto unknown role for STAT1 in promoting gastric disease, since germline deletion of *Stat1* in *gp130*$^{Y757F/Y757}$ mice partially suppressed the growth of gastric tumors concomitant with a reduction in gastric inflammation and STAT3 activation. Collectively, these data implicate IL-11 on a genetic level as the primary cytokine driving gp130-mediated gastric tumorigenesis and provide important evidence for the potential oncogenic cooperation between STAT3 and STAT1 in the progression of inflammation-associated gastric tumors.

Results

Increased expression of IL-6 family cytokines in gastric tumors of gp130$^{Y757F/Y757F}$ *mice.* Elevated expression of IL-11 in human gastric adenocarcinomas (tumors) has recently led to the proposal that IL-11 may serve as a potential biomarker and oncogenic stimulus for human GC (17). We therefore quantified IL-11 expression in tumor-bearing antral tissues from adult *gp130*$^{Y757F/Y757F}$ mice (between 10 and 14 weeks of age) by quantitative RT-PCR and immunoblot analyses. Gastric IL-11 mRNA and protein levels were elevated approximately 30-fold and 15-fold, respectively, in tumors of *gp130*$^{Y757F/Y757F}$ mice compared with unaffected tissue from *gp130*$^{+/+}$ wild-type mice (Figure 1, A and B). Meanwhile, gene expression for the gp130-acting cytokines IL-6 and LIF was elevated by only 5-fold in these lesions (Figure 1A). By contrast, expression of the ligand-specific receptor α-subunits IL-6Rα and IL-11Rα, as well as of the β-subunit gp130, in gastric tissue

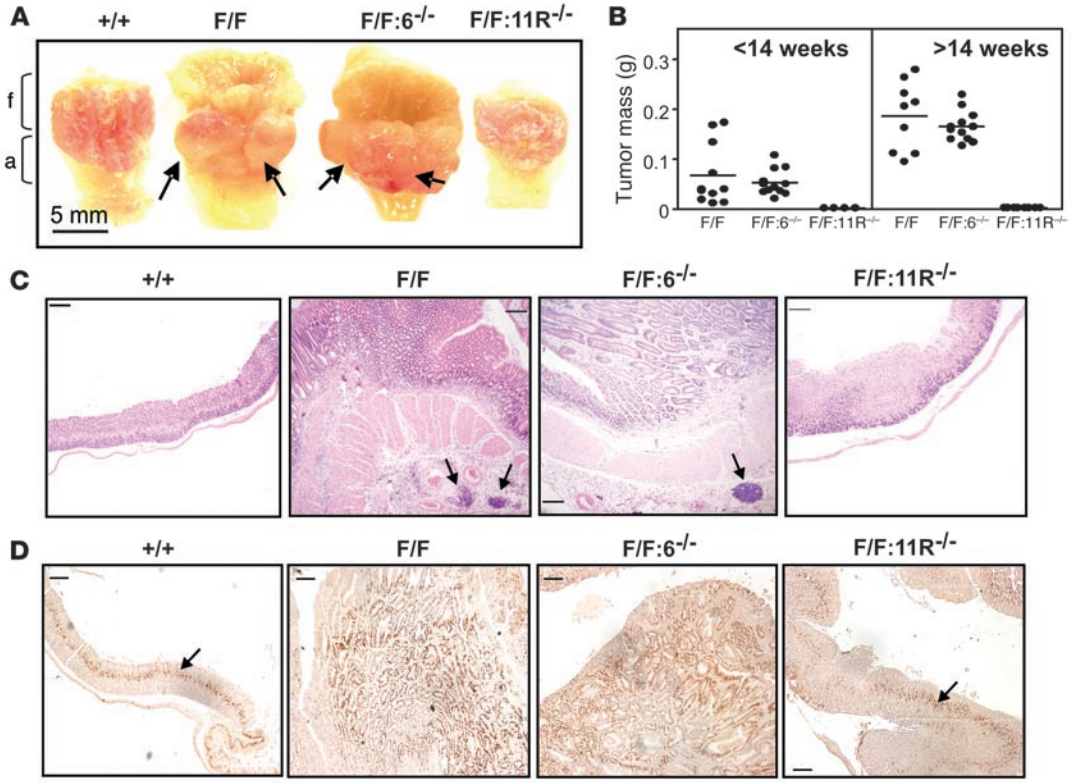

Figure 2
Complete abrogation of gastric tumor formation in *gp130*$^{Y757F/Y757F}$ mice lacking the IL-11Rα1 subunit. (**A**) Representative appearance of stomachs from 14-week-old mice. Stomachs were opened along the outer curvature and pinned out with the lumen facing the viewer. Arrows indicate macroscopically visible lesions. Fundic (f) and antral (a) stomach regions are labeled. (**B**) Scatter plots depicting the total mass (g) of gastric tumors for individual mice either younger or older than 14 weeks of age and belonging to the indicated genotypes. Representative H&E- (**C**) and proliferating cell nuclear antigen–stained (**D**) cross-sections through the antral region of stomachs from mice of the indicated genotypes; arrows indicate patches of inflammatory cell accumulates (**C**) and the defined zone of proliferating mucous neck cells of the gastric epithelium (**D**). Scale bars: 100 μm. F/F: 11R$^{-/-}$ indicates *gp130*$^{Y757F/Y757F}$*Il11ra1*$^{-/-}$ mice; F/F: 6$^{-/-}$ indicates *gp130*$^{Y757F/Y757F}$*Il6*$^{-/-}$ mice.

remained unaffected and was comparable in *gp130*$^{Y757F/Y757F}$ and *gp130*$^{+/+}$ mice (Figure 1C).

IL-11 receptor signaling is essential for gastric tumorigenesis in gp130$^{Y757F/Y757F}$ *mice*. Based on this augmented IL-11 expression in *gp130*$^{Y757F/Y757F}$ gastric tumors (Figure 1, A and B), we explored the notion of a possible causal link between the gastric phenotype and exaggerated signaling emanating from the IL-11 receptor complex. We inactivated IL-11 signaling by generating compound mutant *gp130*$^{Y757F/Y757F}$*Il11ra1*$^{-/-}$ mice, which lack the widely expressed IL-11–specific ligand-binding receptor α-subunit (30), and found that the stomachs of these compound mutant mice were tumor free and indistinguishable in size and cellular morphology from the stomachs of age-matched wild-type mice even when beyond 14 weeks of age (Figure 2, A and B). Notably, gastric sections of *gp130*$^{Y757F/Y757F}$*Il11ra1*$^{-/-}$ mice were characterized by the absence of chronic inflammatory (lymphoplasmacytoid) cell infiltrates in the submucosa and lamina propria (Figure 2C) and did not show any expansion of proliferating (proliferating cell nuclear antigen–positive [PCNA-positive]) gastric cell populations (Figure 2D). By contrast, genetic deletion of *Il6* in *gp130*$^{Y757F/Y757F}$*Il6*$^{-/-}$ mice failed to suppress tumorigenesis (31) and had no ameliorating effect on the inflammatory cell infiltrates and associated gastric hyperplasia characteristically found in *gp130*$^{Y757F/Y757F}$ mice (Figure 2). Collectively, these data identify an essential role for IL-11 receptor–mediated signaling in the initiation and progression of chronic gastritis and gastric adenomatous hyperplasia.

Absence of gastric tumors in gp130$^{Y757F/Y757F}$*Il11ra1*$^{-/-}$ *mice correlates with reduced IL-11 expression and STAT3 activation*. Since genetic reduction of the level of STAT3 activation in *gp130*$^{Y757F/Y757F}$*Stat3*$^{+/-}$ mice impaired the growth of gastric lesions (14), we next investigated whether the extent of gastric STAT3 activation in *gp130*$^{Y757F/Y757F}$ *Il11ra1*$^{-/-}$ mice was affected. Indeed, basal STAT3 tyrosine phosphorylation and expression of the bone fide STAT3 target gene *Socs3* (32) were similar in *gp130*$^{+/+}$ and *gp130*$^{Y757F/Y757F}$*Il11ra1*$^{-/-}$ mice and markedly reduced when compared with those in tumor-bearing *gp130*$^{Y757F/Y757F}$*Il6*$^{-/-}$ and *gp130*$^{Y757F/Y757F}$ mice (Figure 3, A and B). Strikingly, the proportion of phosphorylated STAT3 was less pronounced in the forestomach (fundus) than in the antrum (Figure 3A), and this was reflected by the modest increase in *Socs3* expression observed in the fundus when compared with its antral expression (Figure 3B). Gastric expression of *Il11* mRNA was reduced to wild-type levels in tumor-free *gp130*$^{Y757F/Y757F}$*Il11ra1*$^{-/-}$ mice but remained elevated in *gp130*$^{Y757F/Y757F}$*Il6*$^{-/-}$ mice (Figure 3C). These observations suggest that IL-11 was responsible for gastric STAT3 hyperactivation and that *Il11* may constitute a potential STAT3 target gene (see below) whose augmented expression

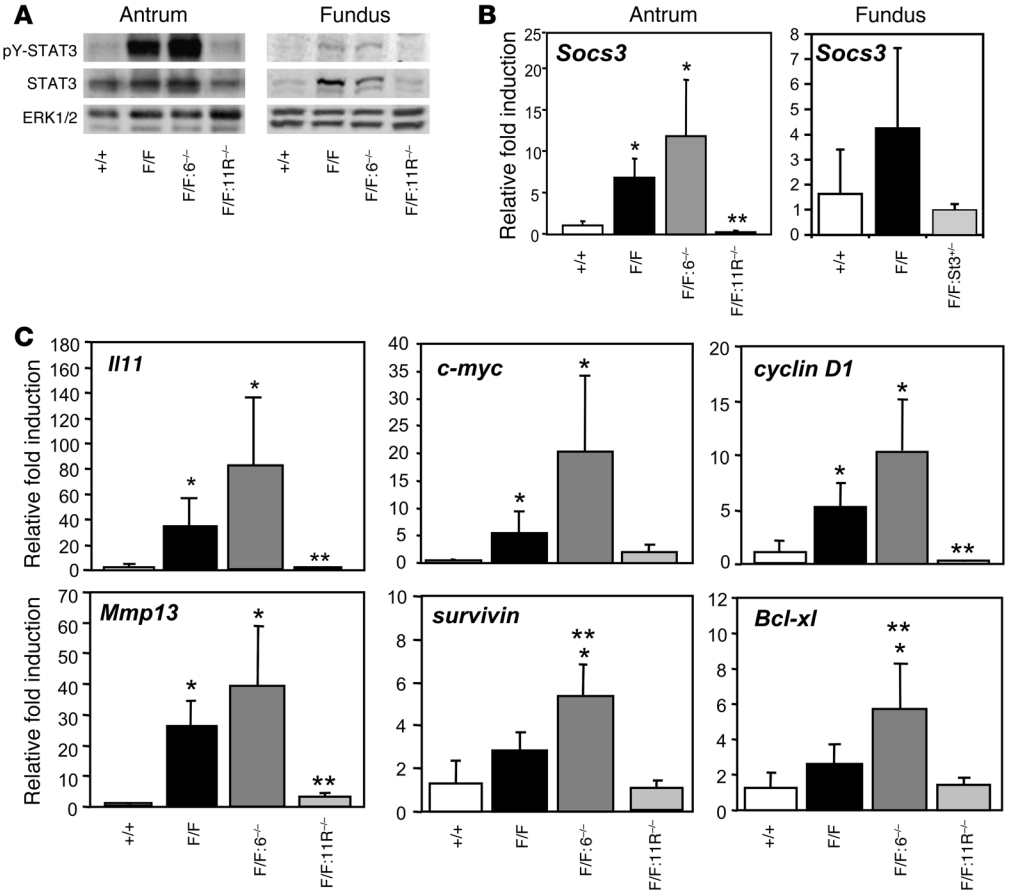

Figure 3

Tumor suppression in *gp130*$^{Y757F/Y757F}$*Il11ra1*$^{-/-}$ mice coincides with reduced IL-11 expression, STAT3 activation, and target gene expression. (**A**) Immunoblot analyses were performed on lysates prepared from antral and fundic gastric tissues of 12- to 14-week-old mice using the indicated antibodies. Q-PCR expression analyses of *Socs3* (**B**) in antral or fundic gastric tissue of the above mice, as well as *Il11* and putative STAT3 target genes (**C**) were performed on cDNA derived from antral tissue of 14-week-old mice of the indicated genotypes. Expression data from 3–5 samples per genotype following normalization for *18S* expression are shown and are presented from replicate analysis as the mean fold induction ± SD relative to expression in *gp130*$^{+/+}$ samples. **P* < 0.05 versus expression in *gp130*$^{+/+}$ samples; ***P* < 0.05 versus expression in *gp130*$^{Y757F/Y757F}$ samples.

correlates with gastric disease. We also observed a tight correlation between the formation of gastric lesions and elevated antral expression of several STAT3 target genes implicated in the pathogenesis of human GC and promoting cellular processes crucial for tumorigenesis, namely cell-cycle progression (*cyclin D1* and *c-myc*) (15), survival (*Bcl-xL* and *survivin*) (12, 14), and extracellular matrix degradation (*Mmp13*) (33) (Figure 3C). Collectively, the above data suggest a compelling correlation among the extent of gastric IL-11 expression, STAT3 phosphorylation, and the expression level of critical STAT3 target genes implicated in tumorigenesis.

Pharmacological interference of STAT3 hyperactivation in gp130$^{Y757F/Y757F}$ *mice reduces gastric tumor burden*. Since our analyses suggest that the IL-11/STAT3 signaling axis contributes to the development of gastric tumors in the *gp130*$^{Y757F/Y757F}$ mouse model, we next explored whether therapeutic targeting of *Stat3* expression (and therefore of its activity) would alleviate established disease. We therefore treated adult *gp130*$^{Y757F/Y757F}$ mice systemically with 2′-methoxyethyl–modified (2′-MOE–modified) antisense oligonucleotides (ASOs) directed against mouse *Stat3* (34). The 2′-MOE modification of the five most 5′ and most 3′ nucleotides provides the STAT3-ASO gapmers with favorable pharmacokinetic characteristics, including suppression of renal clearance due to plasma protein binding and an associated tissue half-life exceeding 14 days (35–37). The physiological responsiveness of individual mice to a 4-week STAT3-ASO treatment regime was confirmed by the rescue of thrombocytosis in *gp130*$^{Y757F/Y757F}$ mice (Figure 4A), since we have previously shown that normal platelet counts are retained throughout the lifetime of *gp130*$^{Y757F/Y757F}$*Stat3*$^{+/-}$ mice (38). Indeed, we observed a dose-dependent reduction in blood platelet counts in STAT3-ASO–treated *gp130*$^{Y757F/Y757F}$ mice to numbers observed in *gp130*$^{+/+}$ mice (15.5×10^8 platelets/ml prior to treatment compared with 6.7×10^8 platelets/ml 2 days after the last ASO treatment; Figure 4A). Importantly, STAT3-ASO treatment also resulted in a smaller overall burden of gastric tumors (Figure 4B) with a reduced abundance of larger (>3 mm in diameter) lesions. Histologically, STAT3-ASO treatment coincided with increased interglandular cell necrosis, fragmentation of glandular (epithelial) structures (Figure 4C), and reduced epithelial staining for the proliferation marker BrdU (Figure 4D).

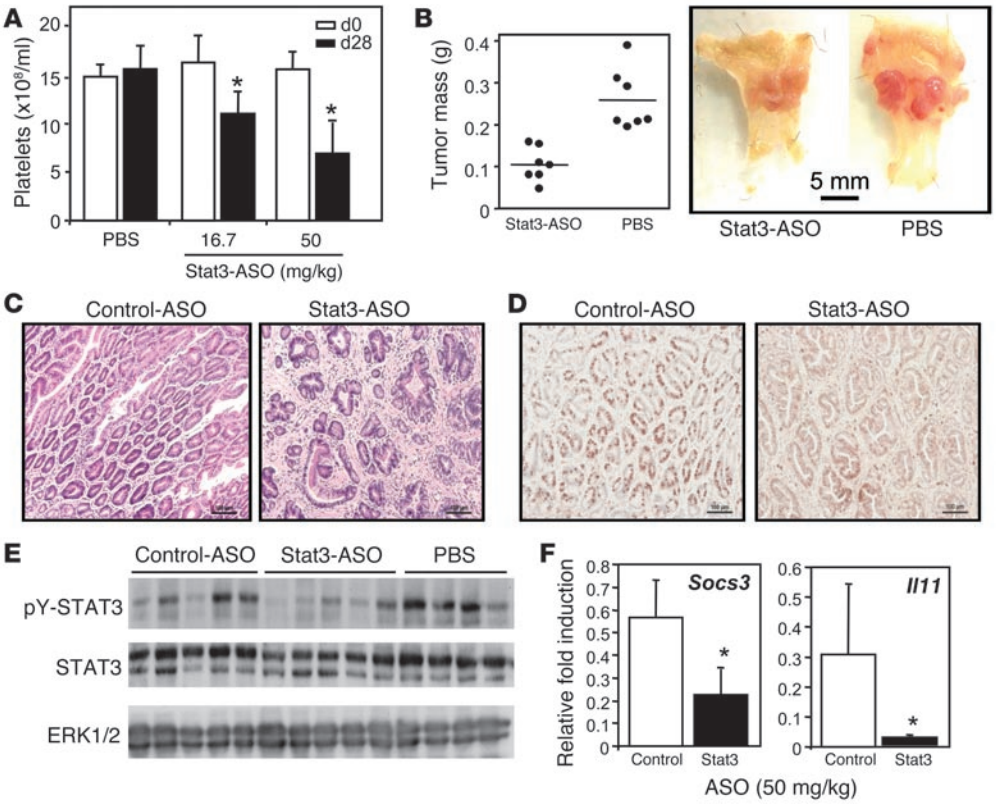

Figure 4
Reduced STAT3 activation and gastric tumor burden in STAT3-ASO–treated *gp130*$^{Y757F/Y757F}$ mice. (**A**) Blood platelet counts of naive adult *gp130*$^{Y757F/Y757F}$ mice treated with either vehicle (PBS) or STAT3-ASO at the indicated concentrations every second day over 28 days. Data are expressed as mean ± SD. $n = 8$ for each treatment group. *$P < 0.05$ versus vehicle-treated mice. (**B**) Representative whole-mount appearance of stomachs from mice shown in **A**. Mice were treated either with vehicle or 50 mg/kg STAT3-ASO. Data points represent the combined wet weight of all excised polyps from individual mice, and the horizontal lines indicate the means. (**C** and **D**) Tissue cross-sections of gastric polyps from mice shown in **B** and stained with either H&E (**C**) or an antibody against BrdU (**D**). Scale bars: 100 μm. (**E**) Immunoblot analyses of antral gastric tissue lysates from individual naive *gp130*$^{Y757F/Y757F}$ mice using the indicated antibodies. Mice were treated with PBS, control-ASO, or STAT3-ASO at a final concentration of 50 mg/kg, and each lane represents an individual mouse. (**F**) Q-PCR analyses of *Socs3* and *Il11* gene expression in gastric tumors from mice shown in **E** and treated with either control ASO or STAT3-ASO at 50 mg/kg. Data are expressed as mean ± SD. $n = 5$ for each treatment group. *$P < 0.05$.

Furthermore, treatment with the STAT3-specific ASO, but not the sequence-scrambled control ASO, resulted in a reduction of total STAT3 expression, with a concomitant reduction in the abundance of phosphorylated STAT3 within the gastric lesions (Figure 4E) and other tissues (data not shown). We also observed reduced expression of the STAT3 target gene *Socs3* as well as of the *Il11* gene in gastric lesions of STAT3-ASO–treated mice (Figure 4F).

STAT3-mediated gastric tumorigenesis is independent of antitumor immunity. While the above data are compatible with a cell-autonomous response of gastric epithelium to STAT3-ASO, tumor-mediated STAT3 hyperactivation in tumor-infiltrating immune cells may inhibit antitumor immunity (39). We therefore assessed cellular localization of activated STAT3 (pY-STAT3) by immunohistochemistry. In stomachs of wild-type mice, pY-STAT3 localized to cells in both the basal portion of the pyloric glands of the antrum and acid-secreting tubules of the corpus, as well as the foveolar epithelium of the gastric antrum and corpus. Although this pattern was retained throughout disease-free regions of stomachs of *gp130*$^{Y757S/Y757F}$ mice, widespread pY-STAT3 immunoreactivity was also observed throughout the epithelial elements of the adenomas and became prominently associated with dense, peritumoral inflammatory cell infiltrates (Figure 5A).

Due to the global presence of the mutation in *gp130*$^{Y757F/Y757F}$ mice and associated STAT3 hyperactivation in hematopoietic cell compartments (29, 36), we next assessed whether the tumor-suppressing effect of STAT3-ASO arose primarily from its activity on gp130-dependent STAT3 hyperactivation in mutant hematopoietic cells. Since 100% of naive *gp130*$^{Y757F/Y757F}$ mice show macroscopically visible gastric lesions by 6 weeks of age (40), we reconstituted lethally irradiated adult *gp130*$^{Y757F/Y757F}$ mice with bone marrow from either eGFP transgene–marked *gp130*$^{+/+}$ mice or autologous *gp130*$^{Y757F/Y757F}$ mice. Two months later, we found nearly complete hematopoietic reconstitution with eGFP-positive *gp130*$^{+/+}$ donor cells, which accounted for greater than 95% of circulating blood cells in these mice (data not shown). Following a further 4-week treatment with STAT3-ASO, we observed a similar reduction in gastric tumor burden in naive *gp130*$^{Y757F/Y757F}$ and reconstituted *gp130*$^{Y757F/Y757F}$ mice, irrespective of the genotype of the donor bone marrow (Figure 5B). These observations therefore suggest that the inhibitory effect of STAT3-ASO on the growth of gastric lesions arises independently

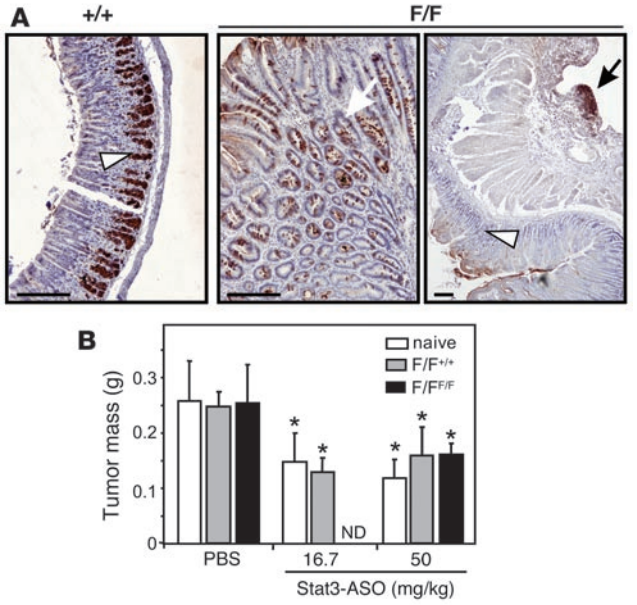

Figure 5
STAT3-dependent gastric tumorigenesis is independent of hematopoietic system–mediated antitumor immunity. (**A**) Immunohistochemical analysis of pY-STAT3 in 12-week-old mice shows staining toward the base of the glandular gastric epithelium in wild-type and unaffected regions in *gp130*$^{Y757F/Y757F}$ mice (arrowheads), with extensive epithelial staining throughout the tumors (white arrow, middle panel) and of submucosal inflammatory cell infiltrates (black arrow, right panel). Scale bars: 100 μm. (**B**) The total wet weight of excised polyps from individual adult *gp130*$^{Y757F/Y757F}$ mice was determined following a 28-day treatment period with PBS vehicle or STAT3-ASO at the indicated concentration. Two months prior to ASO treatment, 6- to 8-week-old mice with established gastric tumors had been reconstituted with either autologous (F/F$^{F/F}$) or heterologous *gp130*$^{+/+}$ bone marrow (F/F$^{+/+}$). Reconstituted mice were approximately 18–20 weeks old when sacrificed, and 12- to 14-week-old *gp130*$^{Y757F/Y757F}$ mice were included to control for potential radiation-mediated alterations to gastric polyp weights. Data are expressed as mean ± SD. $n = 8$ (naive mice), $n = 5$ (reconstituted mice). *$P < 0.05$ versus PBS-treated *gp130*$^{Y757F/Y757F}$ mice belonging to the corresponding group. ND, not determined.

of hematopoietic cells and that maintenance of these tumors is primarily dependent on the continuous availability of hyperactivated STAT3 in nonhematopoietic (i.e., tumor) tissue.

STAT1 hyperactivation contributes to gastric tumorigenesis. We next aimed to genetically dissect the relative contribution of gp130-mediated STAT3 relative to STAT1 hyperactivation to gastric tumorigenesis in *gp130*$^{Y757F/Y757F}$ mice (14). Since there is an absolute requirement for STAT1 to mediate type I and II IFN responses (41), we analyzed stomachs of IFN-responsive *gp130*$^{Y757F/Y757F}$*Stat1*$^{+/-}$ mice (Supplemental Figure 1; supplemental material available online with this article; doi:10.1172/JCI34944DS1), as well as of IFN-unresponsive *gp130*$^{Y757F/Y757F}$*Stat1*$^{-/-}$ mice. Surprisingly, either partial or complete global depletion of the STAT1 pool resulted in stomach sizes in the corresponding compound mutant mice that were noticeably smaller than those of age-matched *gp130*$^{Y757F/Y757F}$ mice (Figure 6A). Furthermore, macroscopically visible tumors were only observed in a proportion of these compound mutant mice when compared with the 100% penetrance of *gp130*$^{Y757F/Y757F}$ mice age 6 weeks or older (Figure 6B). In addition, the abundance of CD45-positive inflammatory cells was reduced in interglandular spaces and submucosal aggregates in stomachs of *gp130*$^{Y757F/Y757F}$*Stat1*$^{+/-}$ and *gp130*$^{Y757F/Y757F}$*Stat1*$^{-/-}$ mice compared with *gp130*$^{Y757F/Y757F}$ mice (Figure 6, C and D) and reminiscent of our previous observation in *gp130*$^{Y757F/Y757F}$*Stat3*$^{+/-}$ mice (42). While the complete absence of functional STAT1 protein in *gp130*$^{Y757F/Y757F}$ *Stat1*$^{-/-}$ mice failed to alleviate tumor burden as effectively as after monoallelic *Stat3* inactivation in *gp130*$^{Y757F/Y757F}$*Stat3*$^{+/-}$ mice (Figure 6, A and B), these data further support a correlation between the presence of inflammatory infiltrates and the occurrence of gastric lesions in *gp130*$^{Y757F/Y757F}$ mice.

To begin to explore the hierarchical relationship between STAT3- and STAT1-dependent mechanisms underlying gastric disease in *gp130*$^{Y757F/Y757F}$ mice, we compared gastric expression of (tumor-associated) STAT3 and STAT1 target genes. Surprisingly, depletion of STAT1 in *gp130*$^{Y757F/Y757F}$*Stat1*$^{-/-}$ mice reduced basal *Stat3* expression and activation (i.e., phosphorylation; Figure 7A). This observation is likely to be of functional significance, because reduced STAT3 phosphorylation in *gp130*$^{Y757F/Y757F}$*Stat1*$^{-/-}$ mice correlates with reduced expression of the STAT3 target genes *Socs3*, *cyclin D1*, *survivin*, and *Mmp13* (Figure 7B). In addition, we found reduced expression of *Il11* and the anticytostatic TGF-β signaling inhibitor *Smad7* in gastric lesions of *gp130*$^{Y757F/Y757F}$*Stat1*$^{-/-}$ mice when compared with *gp130*$^{Y757F/Y757F}$ mice. However, the complete absence of STAT1 was often less effective in reversing enhanced expression of STAT3 target genes in *gp130*$^{Y757F/Y757F}$ mice than observed following monoallelic ablation of *Stat3*. Although genetic restriction of the pool of cellular STAT3 in *gp130*$^{Y757F/Y757F}$*Stat3*$^{+/-}$ mice also reduced basal STAT1 expression and activation (albeit to a lesser extent than observed in the reciprocal situation; Figure 7C), we observed impaired basal expression of the STAT1 target genes *2′-5′-Oas* and *Ip10* (Figure 7D). Collectively, these data are suggestive of a mechanism whereby the level of gp130-dependent activation of STAT3 and to a lesser extent STAT1 functionally mediates and determines the extent of IL-11–driven gastric disease.

STAT1- and STAT3-mediated transcriptional activation of Il11. Since the above data reveal a correlation between the basal activation levels of STAT1 and STAT3 and expression of *Il11* in gastric lesions of *gp130*$^{Y757F/Y757F}$ mice, we next examined whether experimentally biased activation of either STAT1 (by IFN-α) or STAT3 (by IL-11) would directly promote *Il11* expression in vivo. As expected, administration of IFN-α to *gp130*$^{+/+}$ mice predominantly activated the prototypical STAT1-response gene *2′-5′-Oas*, while IL-11 primarily induced the STAT3-response gene *Socs3* (Figure 8A). Gastric *Il11* expression was strongly induced by IL-11, and to a lesser degree after IFN-α administration. The relative potency of response between the 2 cytokines correlated with their capacity to promote STAT3 tyrosine phosphorylation (Figure 8B), and the observed residual STAT3 activation by IFNs was consistent with previous reports (43, 44). Consistent with constitutively elevated activation of STAT3 (and to a lesser extent of STAT1) in *gp130*$^{Y757F/Y757F}$ mice, gastric lesions from these unchallenged mice also showed elevated expression of *Socs3* and *Il11*, as well as a trend for increased *2′-5′-Oas* expression.

In order to further characterize a potential autocrine signaling mechanism by IL-11, we tested the responsiveness of a 1.5-kb frag-

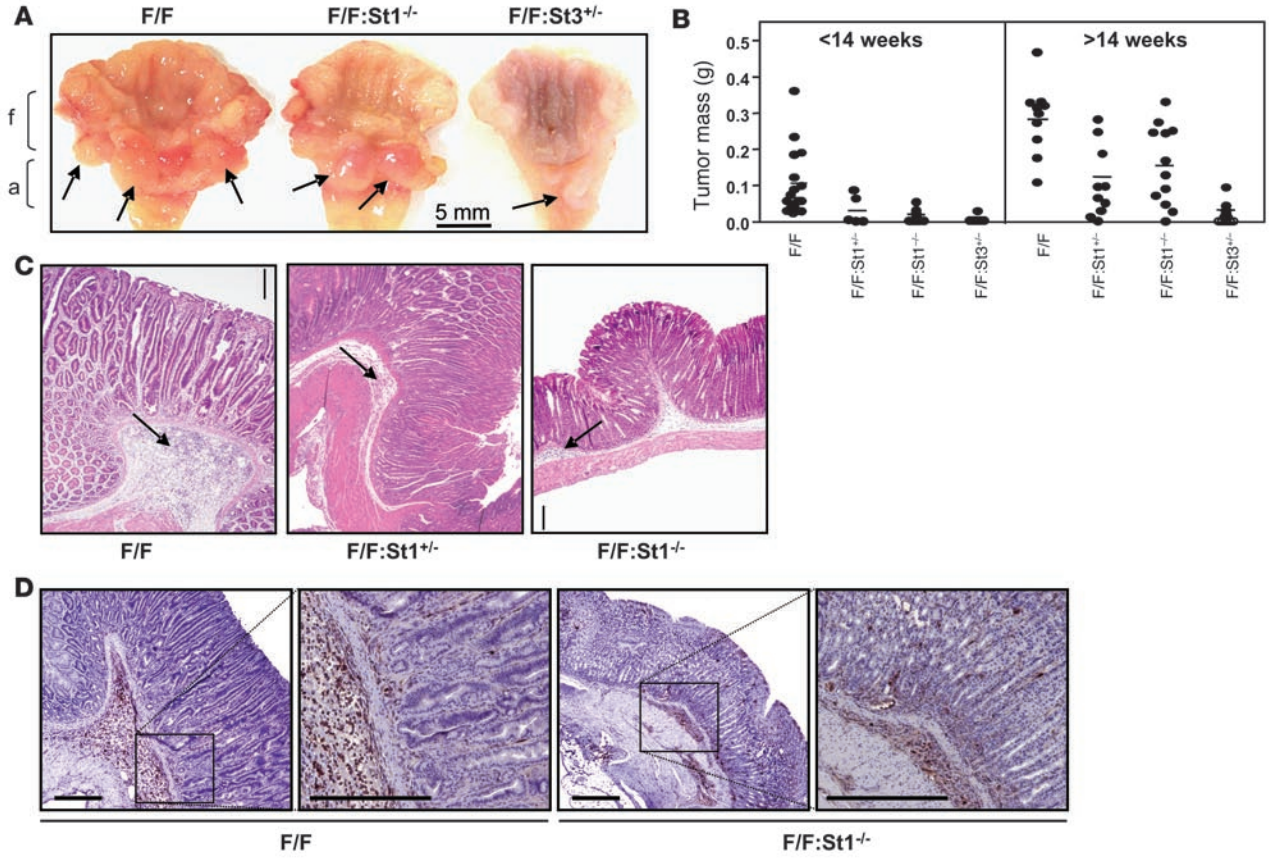

Figure 6
Loss of STAT1 or STAT3 alleles in *gp130*$^{Y757F/Y757F}$ mice alleviates gastric tumor growth. (**A**) Representative appearance of stomachs from 20-week-old mice belonging to the indicated genotypes. Arrows indicate macroscopically visible lesions in the antral but not the fundic regions of stomachs. (**B**) Scatter plots depicting total mass of gastric tumors from individual mice of the indicated genotypes and assessed in 2 different age groups. (**C**) Representative H&E-stained cross-sections through stomachs from 14-week-old mice of the indicated genotypes. (**D**) Representative immunohistochemical staining for CD45-positive hematopoietic cells in stomach sections from 14-week-old mice of the indicated genotypes. Scale bars in all histological sections: 100 μm. FF: St1$^{+/-}$ indicates *gp130*$^{Y757F/Y757F}$*Stat1*$^{+/-}$ mice.

ment upstream of exon 1 of the *Il11* gene promoter. We transiently expressed the corresponding *pIL-11-luc* reporter construct in wild-type mouse embryonic fibroblasts (MEFs) exposed to IFN-α (which activates STAT1 and STAT2), IFN-γ (which only activates STAT1), or the designer cytokine ^{HYPER}IL-6, comprising a fusion protein of IL-6Rα and IL-6 (which activates STAT3 and STAT1). Transfections were also performed in parallel using the STAT-specific reporter constructs *pISRE-luc* and *pAPRE-luc* to monitor for specificity of transactivation by STAT1 and STAT3, respectively. Since stimulation with all 3 cytokines induced *IL-11–luc* activity but only resulted in reciprocal activation of 1 of the 2 STAT-specific reporters (Figure 8C), we conclude that *Il11* can serve as a direct target for STAT3 and to a lesser extent for STAT1. Indeed, nucleotide inspection of the murine *Il11* promoter reveals three 5′-GACN$_3$GAA and one 5′-ATCN$_3$GAA sequence responsive to IL-6/STAT3 signaling and corresponding to sites II and III in the γ-*fibrinogen* gene (45), as well as one 5′-TTAN$_3$GAA sequence responsive to STAT1 (46) (Figure 8D). Collectively, these data suggest the existence of a positive feedback signaling loop whereby IL-11–mediated hyperactivation of STAT3 and STAT1 in *gp130*$^{Y757F/Y757F}$ mice augments the transcriptional activation of *Il11*.

Discussion

The *gp130*$^{Y757F/Y757F}$ mouse is a validated, reproducible, and genetically defined model for gastric tumorigenesis and shares many of the histological hallmarks of inflammation-associated intestinal-type GC in humans (14, 27, 40). Here, we extend the characterization of the *gp130*$^{Y757F/Y757F}$ mouse as an informative preclinical disease model by providing genetic proof for IL-11's pivotal role in mediating aberrant STAT3 and STAT1 activation. In turn, aberrant activation of these latent transcription factors promotes atrophic gastritis that culminates in dysplastic and frequently metaplastic epithelial transformation and the outgrowth of distinct adenomatous polyps (27, 40). Furthermore, we demonstrate in an endogenous tumor model, for the first time to our knowledge, that therapeutic interference aimed at reducing the pool of systemic STAT3 available for activation ameliorates gastric tumor burden. This mechanistic insight is likely to be of clinical relevance, since recurring characteristics of human GC include elevated *Il11* expression (47) and aberrant STAT3 activation, the latter being associated with poor patient survival outcome (11, 48).

The shared use of gp130 as the receptor signaling subunit for an entire family of cytokines together with the "silent" nature of the

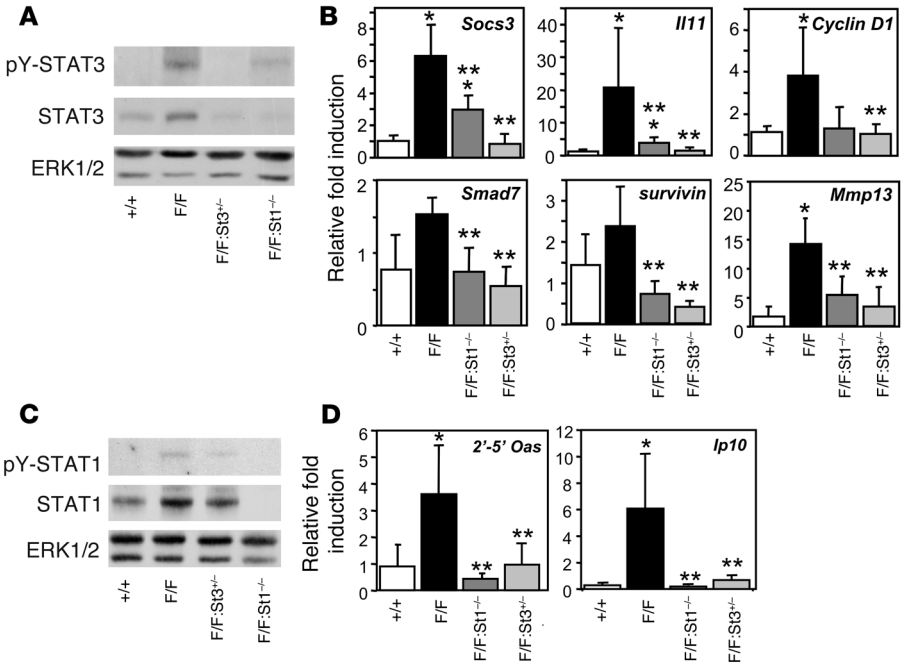

Figure 7
Genetic restriction of STAT1 or STAT3 expression in *gp130*$^{Y757F/Y757F}$ mice coincides with reciprocal reduction in gastric STAT activation and associated target gene expression. (**A** and **C**) Immunoblot analysis of antral gastric tissue lysates from 14-week-old mice of the indicated genotypes using antibodies specific for total ERK1/2, STAT1, or STAT3 and their corresponding tyrosine-phosphorylated forms. (**B** and **D**) Q-PCR analysis of gene expression on antral gastric tissue cDNA prepared from 14-week-old mice. Expression data from 3–5 mice per genotype following normalization for *18S* expression are shown and are presented from replicate analysis as the mean fold induction ± SD relative to expression in *gp130*$^{+/+}$ samples. *$P < 0.05$ versus expression in samples from *gp130*$^{+/+}$ mice. **$P < 0.05$ versus expression in samples from *gp130*$^{Y757F/Y757F}$ mice.

Y757F substitution mutation in the absence of ligand has made it difficult to assign individual cytokines to specific pathologies in *gp130*$^{Y757F/Y757F}$ mice. Our findings that the genetic absence of functional IL-6 or IL-11 signaling in *gp130*$^{Y757F/Y757F}$ mice selectively suppresses the development of a systemic pan-inflammatory response or gastric inflammation–associated tumorigenesis, respectively, enables experimental compartmentalization of phenotypes in the corresponding compound mutant mice. Strikingly, *gp130*$^{Y757F/Y757F}$*Il11ra1*$^{-/-}$ mice lacked inflammatory cell infiltrates in the stomach despite their persistent presence throughout most other organs, including liver, lung, and kidney (B.J. Jenkins and M. Ernst, unpublished observations). Conversely, despite the general absence of inflammatory cells from the latter organs in *gp130*$^{Y757F/Y757F}$*Il6*$^{-/-}$ mice (B.J. Jenkins and M. Ernst, unpublished observations), submucosal infiltrates remained associated with the gastric tumors in these mice. These findings not only highlight the specific requirement of IL-11 to promote and maintain gastric inflammation, but they are also indicative of a causal link between chronic gastric inflammation and tumor formation in the *gp130*$^{Y757F/Y757F}$ model. Indeed, we have previously observed that administration of broad-spectrum antimicrobials to *gp130*$^{Y757F/Y757F}$ mice after weaning reduced tumor growth (42). However, reciprocal bone marrow transfer experiments also showed that gastric accumulation of bone marrow–derived *gp130*$^{Y757F/Y757F}$ cells was insufficient to promote gastric tumorigenesis in wild-type hosts (14). Collectively, these findings lead us to propose that submucosal foci of inflammatory cells either directly supply, or induce localized production of, IL-11. In addition, within the gastric mucosa of *gp130*$^{Y757F/Y757F}$ mice, excessive IL-11–dependent STAT3 hyperactivation then promotes the growth of tumors that have been initiated as a consequence of biasing gp130 signaling toward STAT at the expense of engaging the Shp2/Ras/ERK cascade (14, 27).

Despite the overwhelming evidence for an involvement of STAT3, and to a lesser extent STAT1, in many different types of human malignancies, no activating mutations have been identified in these *STAT* genes. Aberrant activation of the corresponding proteins, however, coincides with (and possibly results from) a variety of other genetic or biochemical alterations. For instance, overproduction and supply of ligand, mutations in receptor and (receptor-associated) cytoplasmic tyrosine kinases, or (epi-)genetic silencing of their negative regulators (15) account for events upstream of STATs that result in their persistent activation. Meanwhile, inappropriate expression of STAT-interacting proteins that alter the transcription-inducing activity of STATs (49), negative regulators of STAT dimerization (50), or STAT dephosphorylation (51) can modify the capacity of STATs to induce target gene expression. On the other hand, genetic data from mice suggest that normal physiological responses are unaffected by partial depletion of the cellular STAT pools in the corresponding heterozygous knockout animals. Collectively, these data suggest the likelihood a favorable therapeutic window to target disease-associated STAT hyperactivation in humans.

Here, we present evidence that therapeutic interference with STAT3 expression reduced the pool of endogenous STAT3 available for activation and ameliorated two of the *gp130*$^{Y757F/Y757F}$ mouse model's independent disease phenotypes, namely thrombocytosis and inflammation-associated gastric tumorigenesis. It has been suggested that targeting STAT3 not only interferes with its cancer cell–autonomous properties, which is attributable to transcriptional induction of genes that promote cell-cycle progression, survival, and angiogenesis (15), but also elicits a potent "bystander" effect by inducing death of tumors cells that have not been reached by STAT3 inhibitors (39). The mechanism underlying this observation relates to the finding that constitutive STAT3 activity in tumor cells promotes immune evasion by tumor-specific production of cytokines (including IL-6 and IL-10) that activate STAT3 in adjacent stroma and cells of the immune system. In a tumor xenograph model, for instance, the immunosuppressive effect of aberrant STAT3 activation was particularly evident on tumor-infiltrating immune cells (e.g., dendritic cells, T cells, NK cells,

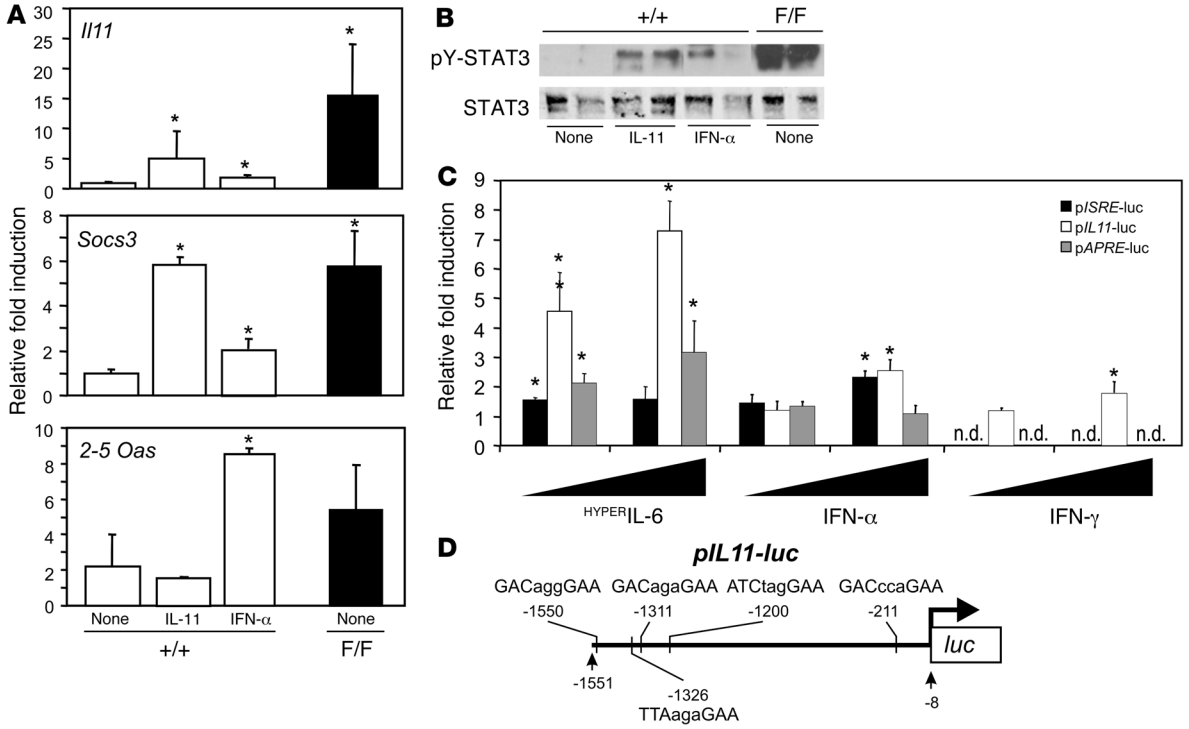

Figure 8

STAT3 and STAT1 induce gastric IL-11 gene expression. (**A**) Q-PCR on antral gastric cDNA prepared from untreated *gp130*$^{Y757F/Y757F}$ mice, as well as *gp130*$^{+/+}$ mice either untreated or injected with a single dose of recombinant IL-11 or IFN-α. Expression data following normalization for *18S* expression are shown and are presented from replicate analysis as the mean fold induction ± SD relative to expression in *gp130*$^{+/+}$ samples. *n* = 3 mice per genotype and treatment. **P* < 0.05 versus expression in untreated *gp130*$^{+/+}$ samples. (**B**) Immunoblot analysis of total STAT3 and tyrosine-phosphorylated STAT3 in antral gastric tissue lysates from mice shown in **A**. (**C**) Transcriptional activation of the mouse *Il11* gene in wild-type MEFs following transient transfection of the *pIL11-luc* firefly luciferase reporter construct. Triplicate cultures of cells, cotransfected with *pTK-RL*, were stimulated with the indicated amount of recombinant IFN-α, IFN-γ, or ^{HYPER}IL-6. Luciferase activity was determined 48 hours later and normalized against activity of the *Renilla* luciferase reporter and expressed relative to unstimulated control cultures. *pAPRE-luc* and *pISRE-luc* transfectants were used to assess for specific STAT3- and STAT1-mediated reporter activation. Data are representative of replicate analyses and are expressed as means of fold changes relative to unstimulated controls ± SD. **P* < 0.05 versus expression in unstimulated cultures. (**D**) Schematic representation of *pIL11-luc* reporter plasmid depicting positions of potential STAT3 (top) and STAT1 (bottom) binding sites relative to the 5′ end of exon 1 of the mouse *Il11* gene. The palindromic core motifs of the STAT binding sites are indicated in upper-case letters, and spacer sequences are indicated in lower-case letters.

neutrophils) and the tumor-specific adaptive immune responses (52). Consequently, ablation or inhibition of STAT3 activity in host hematopoietic cells restored antitumor immunity (39). However, our observations that STAT3-ASO treatment resulted in reduced gastric tumor burden in *gp130*$^{Y757F/Y757F}$ mice irrespective of whether their immune cells carried the gp130(Y757F) mutation suggests a mechanism whereby the therapeutic benefit of STAT3 inhibition is unlikely to be mediated exclusively by an antitumor immune response. Indeed, the adaptive immune system appears to have a negligible effect on progression of tumorigenesis in *gp130*$^{Y757F/Y757F}$ mice, since the appearance of gastric lesions remained largely unaltered when these mice were crossed onto a Rag1-deficient background (31). Furthermore, STAT3 hyperactivation in the *gp130*$^{Y757F/Y757F}$ model promotes rather than suppresses a systemic pan-inflammatory response, which is reminiscent of emerging links between persistent STAT3 activation and inflammation-associated cancers of the liver (53) and colon (54, 55).

Our observation that systemic ablation of *Stat1* ameliorated tumor growth in *gp130*$^{Y757F/Y757F}$ mice is surprising in light of reports that STAT1 mediates IFN-dependent tumor suppressor activity (56) by promoting apoptosis, cell-cycle arrest (57), and tumor surveillance. However, STAT1 is also an essential component in mediating proinflammatory responses, highlighted by findings that IFN treatment rapidly induces gastritis in wild-type mice (58). Similarly, *Socs1*-deficient mice, which are characterized by excessive IFN-dependant STAT1 signaling, spontaneously develop chronic colitis and colorectal carcinomas (59), while antral tumor development in *gastrin*-deficient mice is accompanied by elevated IFN-γ production (60). These observations illustrate the gastrointestinal tract's susceptibility to inflammation-associated tumorigenesis triggered by aberrant IFN signaling and underscore the paradoxical role of the immune system in cancer development (61). While it is unknown whether expression of IL-6 family cytokines is affected in the aforementioned situations, we note that inflammation-dependent colonic tumorigenesis depends on gp130-mediated *trans*-signaling (18). However, our observation that monoallelic *Stat1* ablation reduces tumor burden in the *gp130*$^{Y757F/Y757F}$ background without impairing the IFN-α response of the corresponding MEFs suggests that the tumorigenic activity of STAT1 in *gp130*$^{Y757F/Y757F}$ mice is unlikely

to be related to IFN signaling. On the other hand, the complete absence of *Stat1* in *gp130$^{Y757F/Y757F}$Stat1$^{-/-}$* mice is less effective than monoallelic *Stat3* ablation in *gp130$^{Y757F/Y757F}$Stat3$^{+/-}$* mice, which implies a more prominent role for STAT3/STAT3 homodimers than for the corresponding STAT3/STAT1 heterodimers in mediating the transcriptional response(s) that promote(s) gastric tumorigenesis. At least in intestinal epithelium, however, gp130-dependent STAT1 activation also promotes survival (62). Thus, we propose here that oversupply of the gp130 ligand IL-11 not only induces a STAT3-dependent antiapoptotic, proangiogenic tumor-intrinsic gene expression program, but further fuels continuous gp130 signaling by disproportionate IL-11 expression in response to excessive STAT3 and STAT1 activation. Thus, in addition to targeting STAT3 activation, strategies that antagonize STAT1 may also be of potential therapeutic benefit for the treatment of inflammation-driven cancers characterized by deregulated gp130/STAT3 signaling.

In summary, our genetic dissection demonstrates that persistent IL-11–dependent activation of STAT3, and to a lesser extent of STAT1, specifically promotes inflammation-associated gastric tumorigenesis by a STAT-mediated feed-forward signaling mechanism on the *Il11* gene. Our findings validate, in what we believe to be the first preclinical cancer model of aberrant activation of endogenous STAT3, a concept originating from tumor xenograph models and touting STAT3 as a central signaling node for therapeutic targeting. Hence, the *gp130$^{Y757F/Y757F}$* mouse provides a model for further evaluation and optimization of ASO and complementary strategies embracing small molecules for inhibition of STAT3 activity.

Methods

Mice and treatments. Mice homozygous for the gp130(Y757F) knockin mutation (*gp130$^{Y757F/Y757F}$*), as well as their corresponding compound mutant derivatives lacking either the *Il6* (*gp130$^{Y757F/Y757F}$Il6$^{-/-}$*) or *Il11ra1* (*gp130$^{Y757F/Y757F}$Il11ra1$^{-/-}$*) genes were generated as previously described (30, 31). *gp130$^{Y757F/Y757F}$* mice heterozygous for *Stat3* (*gp130$^{Y757F/Y757F}$Stat3$^{+/-}$*) have previously been reported (14, 36), and mice lacking a functional *Stat1* gene (41) (generously provided by I. Campbell, University of Sydney, Sydney, New South Wales, Australia) were crossed with *gp130$^{Y757F/Y757F}$* mice to generate the compound *gp130$^{Y757F/Y757F}$Stat1$^{-/-}$* and *gp130$^{Y757F/Y757F}$Stat1$^{+/-}$* mutant mice. All animals were housed under specific pathogen–free conditions. All experiments were approved by the Animal Ethics Committee of Monash Medical Centre "A" or the Ludwig Institute for Cancer Research/Department of Surgery Committees and included wild-type (*gp130$^{+/+}$*) littermate controls that were genetically matched.

For cytokine administration, mice were subjected to a single i.p. injection of either human IL-11 (5 μg) or mouse IFN-α (10^5 IU).

For STAT3-ASO treatments, adult *gp130$^{Y757F/Y757F}$* mice with established gastric disease were randomized for sex and placed into the following 3 groups: (a) naive (nonirradiated); (b) lethally irradiated and reconstituted (63) at 6–8 weeks of age with autologous *gp130$^{Y757F/Y757F}$* bone marrow cells (F/F$^{F/F}$); and (c) lethally irradiated and reconstituted (63) with heterologous bone marrow from *gp130$^{+/+}$* mice that carried a TgN(CAG:eGFP) transgene (64) (F/F$^{+/+}$). Naive animals were 12–14 weeks of age upon termination of ASO treatments, while their fully reconstituted counterparts were 18–20 weeks of age. The specificity and pharmacokinetics of the mouse STAT3-ASO (base sequence 5′-AAAAAGTGCCCAGATTGCCC-3′), which hybridized to nucleotides 2,527–2,546 in the 3′ untranslated region, and of the 3-base mismatch (underlined) control ASO (base sequence 5′-AAAAAGAGGCCTGATTGCCC-3′) have been described previously (34). ASOs were dissolved in PBS as vehicle and administered every second day by i.p. injection over a total of 28 days. Blood from the retroorbital plexus of mice was collected into EDTA-coated tubes immediately prior to the first ASO injection and again upon culling mice 2 days after the last ASO administration. Platelet counts were determined on an Advia 120 System quantitative hematology analyzer (Bayer Diagnostics).

Cytokines and antibodies. Recombinant human IL-11 was kindly provided by L. Robb (The Walter and Eliza Hall Institute of Medical Research, Melbourne, Victoria, Australia), while mouse IFN-α1 and human IFN-γ were a gift from N. De Weerd (Monash Institute of Medical Research). The designer cytokine ^{HYPER}IL-6 was kindly provided by S. Rose-John (University of Kiel, Kiel, Germany). Commercially available antibodies against IL-11, gp130, ERK1/2, STAT1, and STAT3 were purchased from Santa Cruz Biotechnology Inc., while phospho(Tyr701)STAT1 and phospho(Tyr705)STAT3 antibodies were from Santa Cruz Biotechnology Inc. and Cell Signaling Technology. Anti-CD45 was from BD Biosciences — Pharmingen.

Cellular assays. To assay for IFN-mediated antiviral cytopathic activity, MEFs generated from day 13 embryos were seeded at 10^4 cells/well in 96-well plates in DMEM containing 10% FBS. Cells were stimulated with varying concentrations of IFN-α and simultaneously challenged with Semliki Forest virus (65) as indicated in Supplemental Figure 1. The extent of IFN-mediated cell survival was assessed by dimethyl thiazole diphenyl tetrazolium bromide (MTT) assay (63).

For luciferase reporter assays, primary MEFs were maintained in DMEM containing 10% FBS and were plated in 24-well plates (5×10^4 cells/well) the day before transfections. Triplicate cultures were transfected (FuGENE 6 reagent; Roche Diagnostics) with the firefly luciferase STAT1 reporter plasmid *pISRE-luc*, the STAT3 reporter plasmid *pAPRE-luc* (14), or the IL-11 reporter plasmid *pIL-11–luc* together with the STAT-independent *Renilla* luciferase plasmid (*pTK-RL*; Promega) to normalize for transfection efficiency. For construction of *pIL-11–luc*, a 1.5-kb fragment immediately upstream of exon 1 of murine *Il11* (ESSEMBL, release 46) was amplified with the sense (5′-CGGGGTACCGGACAGGGAAGGGTTAAAGC) and the antisense primer (5′-GGAAGATCTAGGGAGAAATCAGGCCAAACT), which also included restriction enzyme recognition sites (underlined) in order to enable directional subcloning into the *Kpn*I-*Bgl*II sites of pGL3-Enhancer (Promega). Eight hours after transfection, cells were stimulated with the indicated amounts of either IFN-α or ^{HYPER}IL-6 for 48 hours. Dual luciferase activity was measured using Promega's Dual-Luciferase assay, and firefly activity was normalized to *Renilla* luciferase activity (14).

Histological and immunohistochemical analyses. Following dissection, stomach specimens were fixed in 10% neutral buffered formalin (pH 7.4) solution and embedded in paraffin. For general histology, sections were stained with H&E. Immunohistochemical stainings were performed with antibodies against CD45, pY-STAT3, and PCNA (Dako) on sections from untreated mice. Cellular proliferation was also assessed by staining with an anti-BrdU antibody (BD Biosciences — Pharmingen) of tissues collected 4 hours after injection of 50 μg/kg BrdU (Amersham Biosciences; GE Healthcare). In each case, immunoperoxidase staining was detected with the Liquid Diaminobenzidine (DAB) Substrate Chromogen System (Dako), and sections were counterstained with hematoxylin.

Gastric polyps (tumors) were classified and enumerated according to their size, excised to determine their wet weight, and either snap frozen for RNA/protein analysis or formalin fixed for histological and immunohistochemical analysis.

Protein extraction and immunoblot analysis. Lysates were prepared from snap-frozen gastric tissue in ice-cold lysis buffer, after which they were subjected to immunoblot analyses with the indicated primary antibodies as previously described (63). Proteins were visualized using either

the enhanced chemiluminescence (ECL) detection system (Amersham Biosciences; GE Healthcare) or Odyssey Infrared Imaging System (LI-COR Biosciences) with the appropriate secondary antibodies as per the manufacturer's instructions.

RNA isolation and quantitative expression analysis. Total RNA was extracted from snap-frozen tissues using TRIzol reagent (Invitrogen) according to the manufacturer's protocol. To eliminate any contaminating genomic DNA, on-column DNase digestion was performed using the RNeasy Mini Kit (QIAGEN). cDNA was prepared from 1 μg of total RNA using the SuperScript III First-Strand Synthesis System (Invitrogen) as per the manufacturer's instructions.

Quantitative RT-PCR gene expression analyses were performed on triplicate samples with SYBR Green (Invitrogen) using the 7900HT Fast RT-PCR System (Applied Biosystems) over 40 cycles (95°C/15 s, 60°C/1 min), following an initial denaturation step at 95°C/10 min. Primers to specifically amplify *18S* were used to normalize cDNA concentrations of target genes. Data acquisition and analyses were performed with Sequence Detection System version 2.3 software (Applied Biosystems). Sequences for the mouse primer sets used are provided in Supplemental Table 1.

Statistics. Comparisons between mean values were performed using ANOVA and 2-tailed Student's *t* tests as appropriate. A *P* value of less than 0.05 was considered statistically significant.

Acknowledgments

We thank Val Feakes for expert technical assistance. We are also grateful to Tony Burgess for critical reading of the manuscript. B.J. Jenkins is supported by both an RD Wright Biomedical Fellowship awarded by the National Health and Medical Research Council of Australia (NHMRC) and a Monash University Fellowship. M. Ernst and P.J. Hertzog are supported by a Senior Research Fellowship and Senior Principal Research Fellowship, respectively, from the NHMRC. This work was supported in part by research grants from the NHMRC awarded to B.J. Jenkins, P.J. Hertzog, and M. Ernst.

Received for publication January 7, 2008, and accepted in revised form March 19, 2008.

Address correspondence to: Matthias Ernst, Ludwig Institute for Cancer Research, PO Box 2008, Royal Melbourne Hospital, Victoria 3050, Australia. Phone: 61-3-9341-3155; Fax: 61-3-9341-3104; E-mail: Matthias.Ernst@ludwig.edu.au. Or to: Brendan J. Jenkins, Centre for Functional Genomics and Human Disease, Monash Institute of Medical Research, Monash University, 27-31 Wright Street, Clayton, Victoria 3168, Australia. Phone: 61-3-9594-7218; Fax: 61-3-9594-7211; E-mail: Brendan.Jenkins@med.monash.edu.au.

1. Parkin, D.M., Bray, F., Ferlay, J., and Pisani, P. 2005. Global Cancer Statistics, 2002. *CA Cancer J. Clin.* **55**:74–108.
2. Uemura, N., et al. 2001. Helicobacter pylori infection and the development of gastric cancer. *N. Engl. J. Med.* **345**:784–789.
3. Wang, J.Y., et al. 2001. Mutations of p53 gene in gastric carcinoma in Taiwan. *Anticancer Res.* **21**:513–520.
4. Park, W.S., et al. 2000. Somatic mutations of the trefoil factor family 1 gene in gastric cancer. *Gastroenterology.* **119**:691–698.
5. Guilford, P., et al. 1998. E-cadherin germline mutations in familial gastric cancer. *Nature.* **392**:402–405.
6. Rocco, A., et al. 2006. Gastric adenomas: relationship between clinicopathological findings, Helicobacter pylori infection, APC mutations and COX-2 expression. *Ann. Oncol.* **17**(Suppl. 7):vii103–vii108.
7. Takaku, K., et al. 1999. Gastric and duodenal polyps in Smad4 (Dpc4) knockout mice. *Cancer Res.* **59**:6113–6117.
8. Xu, X., et al. 2000. Haploid loss of the tumor suppressor Smad4/Dpc4 initiates gastric polyposis and cancer in mice. *Oncogene.* **19**:1868–1874.
9. Massague, J., Blain, S.W., and Lo, R.S. 2000. TGF-beta signaling in growth control, cancer, and heritable disorders. *Cell.* **103**:295–309.
10. Boivin, G.P., et al. 1996. Gastric lesions in transforming growth factor beta-1 heterozygous mice. *Lab. Invest.* **74**:513–518.
11. Gong, W., et al. 2005. Expression of activated signal transducer and activator of transcription 3 predicts expression of vascular endothelial growth factor in and angiogenic phenotype of human gastric cancer. *Clin. Cancer Res.* **11**:1386–1393.
12. Kanda, N., et al. 2004. STAT3 is constitutively activated and supports cell survival in association with survivin expression in gastric cancer cells. *Oncogene.* **23**:4921–4929.
13. Kanai, M., et al. 2003. Differentiation-inducing factor-1 (DIF-1) inhibits STAT3 activity involved in gastric cancer cell proliferation via MEK-ERK-dependent pathway. *Oncogene.* **22**:548–554.
14. Jenkins, B.J., et al. 2005. Hyperactivation of Stat3 in gp130 mutant mice promotes gastric hyperproliferation and desensitizes TGF-beta signaling. *Nat. Med.* **11**:845–852.
15. Bromberg, J. 2002. Stat proteins and oncogenesis. *J. Clin. Invest.* **109**:1139–1142.
16. Levy, D.E., and Lee, C.K. 2002. What does Stat3 do? *J. Clin. Invest.* **109**:1143–1148.
17. Ellmark, P., et al. 2006. Identification of protein expression signatures associated with Helicobacter pylori infection and gastric adenocarcinoma using recombinant antibody microarrays. *Mol. Cell Proteomics.* **5**:1638–1646.
18. Becker, C., et al. 2005. IL-6 signaling promotes tumor growth in colorectal cancer. *Cell Cycle.* **4**:217–220.
19. Naugler, W.E., et al. 2007. Gender disparity in liver cancer due to sex differences in MyD88-dependent IL-6 production. *Science.* **317**:121–124.
20. Kishimoto, T., Akira, S., Narazaki, M., and Taga, T. 1995. Interleukin-6 family of cytokines and gp130. *Blood.* **86**:1243–1254.
21. Heinrich, P.C., et al. 2003. Principles of interleukin (IL)-6-type cytokine signalling and its regulation. *Biochem. J.* **374**:1–20.
22. Heinrich, P.C., Behrmann, I., Muller-Newen, G., Schaper, F., and Graeve, L. 1998. Interleukin-6-type cytokine signalling through the gp130/Jak/STAT pathway. *Biochem. J.* **334**:297–314.
23. Gerhartz, C., et al. 1996. Differential activation of acute phase response factor/STAT3 and STAT1 via the cytoplasmic domain of the interleukin 6 signal transducer gp130. I. Definition of a novel phosphotyrosine motif mediating STAT1 activation. *J. Biol. Chem.* **271**:12991–12998.
24. Nicholson, S.E., et al. 2000. Suppressor of cytokine signaling-3 preferentially binds to the SHP-2-binding site on the shared cytokine receptor subunit gp130. *Proc. Natl. Acad. Sci. U. S. A.* **97**:6493–6498.
25. Takahashi-Tezuka, M., et al. 1998. Gab1 acts as an adapter molecule linking the cytokine receptor gp130 to ERK mitogen-activated protein kinase. *Mol. Cell. Biol.* **18**:4109–4117.
26. Krebs, D.L., and Hilton, D.J. 2001. SOCS proteins: negative regulators of cytokine signaling. *Stem Cells.* **19**:378–387.
27. Tebbutt, N.C., et al. 2002. Reciprocal regulation of gastrointestinal homeostasis by SHP2 and STAT-mediated trefoil gene activation in gp130 mutant mice. *Nat. Med.* **8**:1089–1097.
28. Laiho, M., et al. 1990. Growth inhibition by TGF-beta linked to suppression of retinoblastoma protein phosphorylation. *Cell.* **62**:175–185.
29. Monteleone, G., et al. 2004. Induction and regulation of Smad7 in the gastric mucosa of patients with Helicobacter pylori infection. *Gastroenterology.* **126**:674–682.
30. Jenkins, B.J., et al. 2007. Pathologic consequences of STAT3 hyperactivation by IL-6 and IL-11 during hematopoiesis and lymphopoiesis. *Blood.* **109**:2380–2388.
31. Howlett, M., et al. 2005. Differential regulation of gastric tumor growth by cytokines that signal exclusively through the coreceptor gp130. *Gastroenterology.* **129**:1005–1018.
32. Maritano, D., et al. 2004. The STAT3 isoforms alpha and beta have unique and specific functions. *Nat. Immunol.* **5**:401–409.
33. Elnemr, A., et al. 2003. Expression of collagenase-3 (matrix metalloproteinase-13) in human gastric cancer. *Gastric Cancer.* **6**:30–38.
34. Chiarle, R., et al. 2005. Stat3 is required for ALK-mediated lymphomagenesis and provides a possible therapeutic target. *Nat. Med.* **11**:623–629.
35. Dean, N.M., and Bennett, C.F. 2003. Antisense oligonucleotide-based therapeutics for cancer. *Oncogene.* **22**:9087–9096.
36. Yu, R.Z., et al. 2004. Tissue disposition of 2'-O-(2-methoxy) ethyl modified antisense oligonucleotides in monkeys. *J. Pharm. Sci.* **93**:48–59.
37. Geary, R.S., et al. 2001. Pharmacokinetic properties of 2'-O-(2-methoxyethyl)-modified oligonucleotide analogs in rats. *J. Pharmacol. Exp. Ther.* **296**:890–897.
38. Jenkins, B.J., Roberts, A.W., Najdovska, M., Grail, D., and Ernst, M. 2005. The threshold of gp130-dependent STAT3 signaling is critical for normal regulation of hematopoiesis. *Blood.* **105**:3512–3520.
39. Kortylewski, M., et al. 2005. Inhibiting Stat3 signaling in the hematopoietic system elicits multicomponent antitumor immunity. *Nat. Med.* **11**:1314–1321.
40. Judd, L.M., et al. 2004. Gastric cancer development in mice lacking the SHP2 binding site on the IL-6 family co-receptor gp130. *Gastroenterology* **126**:196–207.
41. Meraz, M.A., et al. 1996. Targeted disruption of the Stat1 gene in mice reveals unexpected physiologic specificity in the JAK-STAT signaling pathway. *Cell.* **84**:431–442.
42. Judd, L.M., Kalantzis, A., Jenkins, B.J., Ernst, M., and Giraud, A.S. 2006. STAT3 activation regulates growth, inflammation, and vascularization in a

mouse model of gastric tumorigenesis. *Gastroenterology.* **131**:1073–1085.
43. Costa-Pereira, A.P., et al. 2002. Mutational switch of an IL-6 response to an interferon-gamma-like response. *Proc. Natl. Acad. Sci. U. S. A.* **99**:8043–8047.
44. Haan, S., Keller, J., Behrmann, I., Heinrich, P.C., and Haan, C. 2005. Multiple reasons for an inefficient STAT1 response upon IL-6-type cytokine stimulation. *Cell Signal.* **17**:1542–1550.
45. Zhang, Z., Fuentes, N., and Fuller, G.M. 1995. Characterization of the IL-6 responsive elements in the gamma fibrinogen gene promoter. *J. Biol. Chem.* **270**:24287–24291.
46. O'Brien, C.A., and Manolagas, S.C. 1997. Isolation and characterization of the human gp130 promoter. Regulation by STATS. *J. Biol. Chem.* **272**:15003–15010.
47. Nakayama, T., et al. 2007. Expression of interleukin-11 (IL-11) and IL-11 receptor alpha in human gastric carcinoma and IL-11 upregulates the invasive activity of human gastric carcinoma cells. *Int. J. Oncol.* **30**:825–833.
48. Yakata, Y., et al. 2007. Expression of p-STAT3 in human gastric carcinoma: significant correlation in tumour invasion and prognosis. *Int. J. Oncol.* **30**:437–442.
49. Nabarro, S., et al. 2005. Coordinated oncogenic transformation and inhibition of host immune responses by the PAX3-FKHR fusion oncoprotein. *J. Exp. Med.* **202**:1399–1410.
50. Wang, L., and Banerjee, S. 2004. Differential PIAS3 expression in human malignancy. *Oncol. Rep.* **11**:1319–1324.
51. Zhang, X., et al. 2007. Identification of STAT3 as a substrate of receptor protein tyrosine phosphatase T. *Proc. Natl. Acad. Sci. U. S. A.* **104**:4060–4064.
52. Wang, T., et al. 2004. Regulation of the innate and adaptive immune responses by Stat-3 signaling in tumor cells. *Nat. Med.* **10**:48–54.
53. Ogata, H., et al. 2006. Deletion of the SOCS3 gene in liver parenchymal cells promotes hepatitis-induced hepatocarcinogenesis. *Gastroenterology.* **131**:179–193.
54. Atreya, R., et al. 2000. Blockade of interleukin 6 trans signaling suppresses T-cell resistance against apoptosis in chronic intestinal inflammation: evidence in crohn disease and experimental colitis in vivo. *Nat. Med.* **6**:583–588.
55. Rigby, R.J., Simmons, J., Greenhalgh, C.J., Alexander, W.S., and Lund, P.K. 2007. Suppressor of cytokine signaling 3 (SOCS3) limits damage-induced crypt hyper-proliferation and inflammation-associated tumorigenesis in the colon. *Oncogene.* **26**:4833–4841.
56. Kaplan, D.H., et al. 1998. Demonstration of an interferon gamma-dependent tumor surveillance system in immunocompetent mice. *Proc. Natl. Acad. Sci. U. S. A.* **95**:7556–7561.
57. Schroder, K., Hertzog, P., Ravasi, T., and Hume, D.A. 2004. Interferon-gamma: an overview of signals, mechanisms and functions. *J. Leukoc. Biol.* **75**:163–189.
58. Zavros, Y., et al. 2003. Treatment of Helicobacter gastritis with IL-4 requires somatostatin. *Proc. Natl. Acad. Sci. U. S. A.* **100**:12944–12949.
59. Hanada, T., et al. 2006. IFNgamma-dependent, spontaneous development of colorectal carcinomas in SOCS1-deficient mice. *J. Exp. Med.* **203**:1391–1397.
60. Zavros, Y., et al. 2005. Chronic gastritis in the hypochlorhydric gastrin-deficient mouse progresses to adenocarcinoma. *Oncogene.* **24**:2354–2366.
61. de Visser, K.E., Eichten, A., and Coussens, L.M. 2006. Paradoxical roles of the immune system during cancer development. *Nat. Rev. Cancer.* **6**:24–37.
62. Yuan, H., Liddle, F.J., Mahajan, S., and Frank, D.A. 2004. IL6-induced survival of colorectal carcinoma cells is inhibited by butyrate through down-regulation of the IL6 receptor. *Carcinogenesis.* **25**:2247–2255.
63. Jenkins, B.J., et al. 2004. Imbalanced gp130-dependent signaling in macrophages alters macrophage colony-stimulating factor responsiveness via regulation of c-fms expression. *Mol. Cell. Biol.* **24**:1453–1463.
64. Okabe, M., Ikawa, M., Kominami, K., Nakanishi, T., and Nishimune, Y. 1997. 'Green mice' as a source of ubiquitous green cells. *FEBS Lett.* **407**:313–319.
65. Hertzog, P.J., Wright, A., Harris, G., Linnane, A.W., and Mackay, I.R. 1991. Intermittent interferonemia and interferon responses in multiple sclerosis. *Clin. Immunol. Immunopathol.* **58**:18–32.